Optimization of extrudate swell during extrusion-based additive manufacturing process

Abel Cherouat[1, a)], Thierry Barriere [2, b)] and Hong Wang[1, c)]

[1] *Université de Technologie de Troyes, UR-GAMMA3, 12 rue Marie Curie, 10004 Troyes, France*
[2] *Université de Franche-Comté, Institut FEMTO-ST, 1 rue Claude Goudimel, 25000 Besançon, France*

[a)] *Corresponding author: abel.cherouat@utt.fr*
[b)] *thierry.barriere@univ-fcomte.fr*
c) hong.wang@utt.fr

Abstract. *Die swell is the expansion of the extrudate diameter upon exiting the die, resulting from the polymer melt or ink undergoes high shear stress due to the pressure-driven flow, viscoelastic relaxation phenomenon and the molecular chains stretching and oriented in the flow direction. Die swell affects dimensional accuracy and interlayer bonding and it's crucial to understood and controlled for high-precision manufacturing. It can be affected by multiple factors including material properties and processing parameters that can be coupled and it is difficult to fully understand their effects. To minimize or control extrudate swell it is necessary to identify the optimal combination of process parameters using Orthogonal Arrays. In this study, Orthogonal Experimental Design is used to optimize extrudate swell during extrusion-based additive manufacturing MEX of biodegradable polylactic acid material. It allows to systematically investigate the influence of multiple process parameters and their interactions on the swell ratio, using a minimal number of experiments. Simulating swell during extrusion with COMSOL Multiphysics requires combining computational fluid dynamics and Level Set method with rheological modeling of the extruded material. The results and analyses of the numerical simulation were used to predict and optimize the extrudate swelling in the MEX process.*

INTRODUCTION

The extrusion swelling (or die swell) of polymers during extrusion-based additive manufacturing (MEX) refers to the expansion of the polymer filament as it exits the nozzle during extrusion. This critical phenomenon affects print accuracy, dimensional control, and surface quality [1]. Due to viscoelastic nature of the polymer melt accumulated during flow through the nozzle, the polymer chains are stretched and aligned in the flow direction under high shear inside the nozzle and they relaxed elastically at the nozzle exit leading to expansion of the filament diameter. There are three basic mechanisms related to the polymer extrudate swelling:

1) Recombination of the velocity profile at the nozzle outlet due to the disappearance of the wall stress;
2) Elastic recovery of the elongation strain relating to the Deborah number if it is larger than 1;
3) Relaxation of the first shear flow-induced normal stress difference in the shear flow.

Swelling can be affected by multiple factors, such as temperature (higher temperature → lower viscosity → less swell polymer viscosity (higher viscosity → more swelling), nozzle geometry and size (shorter nozzles → less stress relaxation → more swell)low rate / shear rate (high shear rate → more stress → more swell)cooling fans, and polymer molecular weight [2]. Liang et al. [3] used a capillary rheometer to measure the swelling ratio of polypropylene (PP) in the die. By increasing the shear rate, the swelling ratio increased sharply at low shear rate and gradually reached the maximum value at the highest shear rate. When the shear rate was fixed, the swelling ratio decreased with increasing temperature. Anand et al. [4] reported the swelling of molten PP melts with capillary dies of different ratio RGD = length/diameter and show that the swelling decreased with increasing RGD when the shear rate was fixed.

In order to evaluate the extrusion swelling ratio with different RGDs, Behzadfar et al. [5] used a capillary die to measure filament diameter post-deposition vs. nozzle diameter. They show that swelling ratio decreased with increasing RGD and decreased with increasing entrance angle up to 180°. Therefore, controlling die swelling is crucial, especially in applications that require high accuracy, precision of printed parts and dimensional stability. In order to understand the relation of polymer viscoelasticity, processing conditions and die swelling, the experimental data of die swell measure is essential. Early research attempt to measure the extrudate swell with pinch-off method that the extrudate is frozen for measurement [6], [7] and [8]. This method is inaccurate as it involves the error resulting from cooling and solidifying. More accurate methods include the use of in-time equipment like infrared transmission and optical cameras are used [9], [10] and [11]. Train models using experimental data to predict and adjust for swelling dynamically can used to control or minimize die swelling. Computational Fluid Dynamics (CFD)

and rheological modeling can used to simulate the swelling behavior and predict the final dimensions of the extrudate after it exits the nozzle, as well as the profile of pressure, velocity, and temperature along the extrusion path. By modeling the polymer melt behavior, extrusion parameters, and cooling effects, one can reduce errors due to swell and improve print accuracy.

The Phan-Thien–Tanner (PTT) model [12] is a rheological constitutive model used to describe the behavior of viscoelastic polymer melts and solutions, particularly in extensional and shear flows—making it highly suitable for simulating extrusion swelling in polymer-based additive manufacturing. They found that increasing the width / height ratio from 1 to 20 contributed to 10 – 30 % extrudate deformation in different directions and delayed the equilibrium position along the flow direction.

The Kaye–Bernstein–Kearsley–Zapas (K-BKZ) model is an advanced integral-type constitutive model used to describe the nonlinear viscoelastic behavior of polymeric fluids**,** especially in flows involving large deformations such as extrusion and die swell. The Oldroyd-B model is a differential constitutive model used to describe the behavior of viscoelastic fluids**,** such as polymer melts and polymer solutions. It's used to modeling flows where both viscous and elastic effects are significant—such as in MEX.

Konaganti et al. [13] used the K-BKZ model and a differential model (like Maxwell or Oldroyd-B) to investigate the extrudate swell of a molten high-density polyethylene through capillary dies. They show that extrudate swell decreases with increasing temperature, apparent shear rate and the RGD. We can conclude that the K-BKZ model overestimated and the PTT model underpredicted the experimental results, leading to an unexplained problem.

Modern approaches combine experimental**,** theoretical**,** and numerical techniques to better understand, predict, and control this viscoelastic phenomenon. When a viscoelastic polymer melt exits the die nozzle, it tends to expand in cross-section due to the release of stored elastic energy from molecular stretching during flow. This results in a swelling ratio, which must be accurately predicted or minimized for dimensional accuracy.

In this study, an online experimental rheometry and high-Speed Imaging method using a high definition camera and a thermal camera to capture the extrusion swell and temperature distribution downstream of the nozzle exit was adopted. Processing parameters such as temperature, extrusion rate and nozzle diameter of a MEX printer were studied. The experimental results were fed into the Two-Phase Flow (TPF) module of the COMSOL Multiphysics coupling (thermal**,** viscoelastic, and phase transition) and process integration with the Level-Set (LS) method to predicted or minimized for dimensional accuracy.

EXPERIMENTAL CHARACTERIZATION OF EXTRUDATE SWELLING

To characterize the extrudate swelling, a dynamic camera (Basler Ace acA3088) with a frame rate of 25 fps (40 ms/frame) and an infrared camera (Optris PI 450i) with a temperature range of -20 to 900 °C was chosen to quantify the temperature and velocity and the final dimensions of the extrudate profile (see Figure 1).

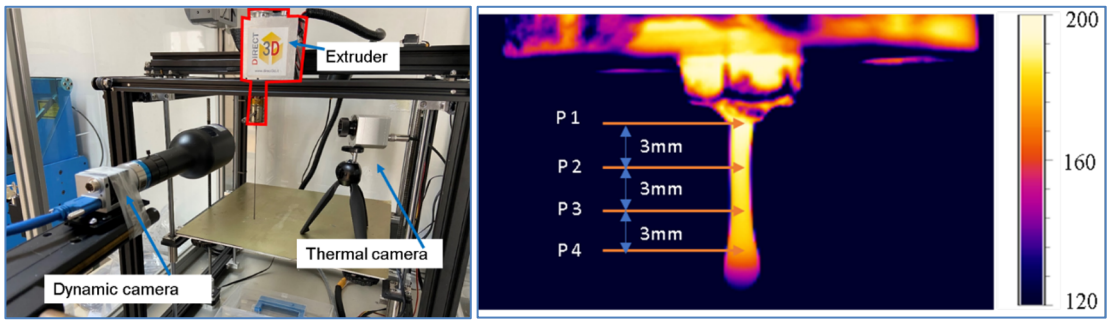

FIGURE 1. Dynamic and the infrared cameras and temperature profile of the extrudate (°C)

The overall procedure for characterizing extrudate swelling is:

A. **Emissivity measure:** The PLA material were placed on a temperature-controlled heating plate and heated to the molten state. The head of a thermocouple was placed on the surface of the molten material to measure the temperature and the emissivity was determined by adjusting the temperature of the infrared camera to match the temperature of the thermocouple. The emissivity of PLA was determined at 0.92, in the range of 0.92 to 0.95 in the literature [14] and [15].

B. **Temperature measure:** A small 3×3 pixels control region was selected near the die exit to measure the temperature of the extrudate and three other areas were selected to evaluate the temperature change with the extrudate, as shown in Figure 2. As the extrudate flowed downward through the observation points (P1-P4), the temperature at each point as a function of time was recorded in real time. The curves can be divided into three domains:

1. Extrudate arrival: the temperature remains room temperature until the extrudate arrives.
2. Unsteady state: represents the temperature variation resulting from the extrusion process in which the newly introduced cooler material exchanges heat or mix with the material ahead of it, as well as the irregular movement of the extrudate front.
3. Steady state: as the higher temperature material heated to a static state is extruded, the temperature evolution becomes stable and the extrudate swell measurement begins in this steady state.

The extrusion temperatures T_{m1} = 190 °C, T_{m2} = 200 °C and T_{m3} = 210 °C were selected in this study to test the stability of the extrusion process without defect. For each extrusion temperature, four extrusion rates (S_1 = 10 rpm, S_2 = 20 rpm, S_3 = 30 rpm and S_4 = 40 rpm) were tested. Two nozzles of length L = 0.6 mm and different diameters ($\varnothing D_1$ = 0.76 mm and $\varnothing D_2$ = 1.56 mm) were studied for optimization and comparison.

C. **Swelling measure:** The images were calibrated in ImageJ software by calculating the ratio of the distance in pixels to the actual distance of the lateral length of an object. The scale was set to 0.012 mm/pixel (1500 / 18 = 82.942 pixels/mm), which corresponds to a negligible measurement error of 1.6%. The images were then converted to black and white binary images and the maximal diameter of the extrudate was measured 2 mm below the nozzle outlet at a flow time of t = 1s to determine the die swell diameter $\varnothing D_e$.

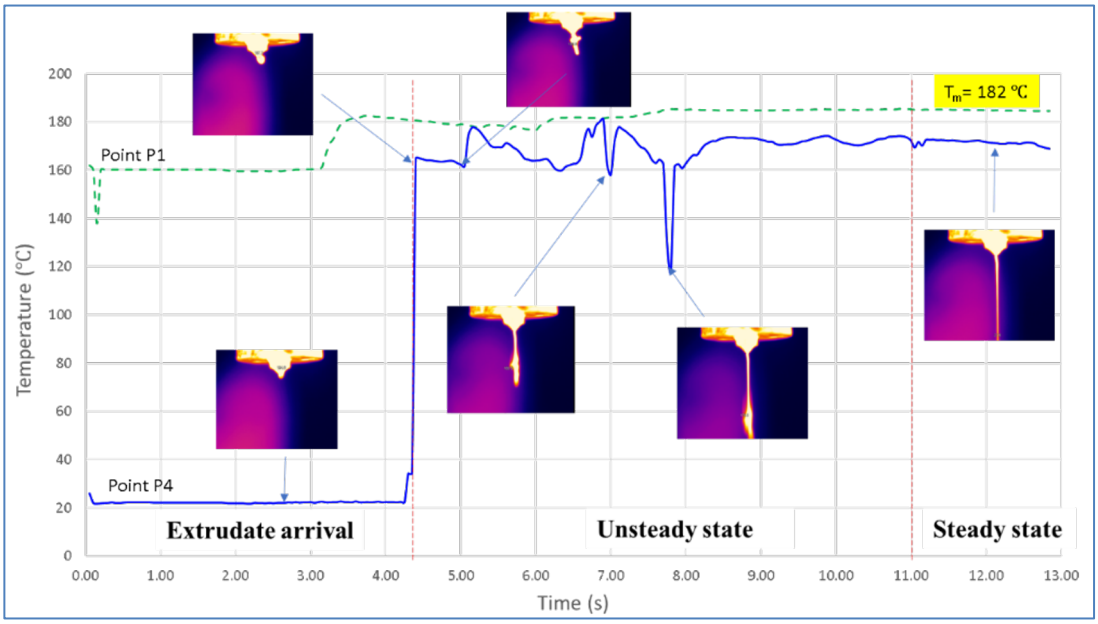

FIGURE 2. Evolution of temperature of PLA flow at T_{m1} and S_4.

ORTHOGONAL EXPERIMENT DESIGN OPTIMIZATION

Orthogonal Experiment Design (OED) is a powerful statistical approach used to optimize processes with multiple parameters while minimizing the number of experiments. It is widely applied in polymer extrusion to optimize and control extrusion swell, especially in additive manufacturing. To optimize extrusion parameters (like extrusion rate S, extrusion temperature T_m and nozzle diameter $\varnothing D$) on exit temperature profile T_s and volume flow rate Q_v in order to minimize extrudate swell, a systematic and efficient orthogonal experiment optimization with 3 factors and 2 levels as shown in Table 1 is used.

TABLE 1. Factors and levels of orthogonal experiment.

Factor	Extrusion rate S (rpm)	Extrusion temperature T_m (℃)	Nozzle diameter ∅D (mm)
-1	10	190	0.76
1	40	210	1.56

TABLE 2. Tests of orthogonal experiment design.

Test	Extrusion rate S (rpm)	Extrusion temperature T_m (℃)	Nozzle diameter ØD (mm)	Exit temperature T_s (℃)	Volume flow rate Q_v (mm^3/s)
1	-1	1	-1	201.50	4.26
2	-1	-1	-1	183.90	3.10
3	1	-1	1	177.10	25.60
4	1	1	1	193.40	34.90
5	-1	-1	1	182.30	6.40
6	1	1	-1	195.33	16.29
7	1	-1	-1	178.30	11.63
8	-1	1	1	199.00	9.69

After performing the 8 experiments to minimize die swell by adjusting temperature, speed, and nozzle geometry measure, the optimal level for each factor are:

A. **Highest exit temperature T_s** is obtained with lower extrusion rate S, higher extrusion temperature T_m, and lower nozzle diameter $ØD$ and their order of effect is $T_m \rightarrow S \rightarrow ØD$. The temperature T_s tends to decrease when extrusion rate S increases, which can be explained by the reduction of the residence time of the material in the heat inside the extrude.

B. **Larger nozzle diameter $ØD$** facilitates the flow of material, which also reduces the residence time inside the extruder and, therefore, a higher temperature T_m can result in a higher T_s. Figure 3 shows the interaction diagram for T_s. The two curves of each combination are parallel, indicating that the interaction effect between the two factors is small or zero. Figure 3(c) shows the main effects plot for Q_v. The highest Q_v is obtained when all factors are at their highest value and their order of effect is $S \rightarrow ØD \rightarrow T_m$. The feeding process is a confrontation process of the shear force driven by screw against the force due to the pressure drop inside the nozzle.

C. **Higher $ØD$** and **higher T_m** can decrease the shear resistance, which reduces the pressure drop, while higher S induces higher shear forces in the material flow, which allows for faster material feeding. Hyvärinen et al. [16] reported that Q_v tends to decrease with S due to increased slip at the screw, which was not detected in this study. Figure 3(d) shows the interaction curve for Q_v. The curve has different slops but with the same trend, indicating that the interaction effect of S*T_m, S*D and T_m*D is moderate. This also proves that the highest Q_v is obtained when the higher level of each factor in their interactions is selected. For both responses, the S*T_m*D interaction is neglected.

The regression equations for exit temperature T_s and volumetric flow rate Q_v were obtained as a function of studied factors and their interactions, with R^2 = 100% and 99.36%, respectively:

$$\begin{cases} T_s = 188.80 - 2.82S + 8.45T_m - 0.90D - 0.12ST_m + 0.12SD - 0.20T_mD \\ Q_v = 13.99 + 8.12S + 2.30T_m + 5.16D + 1.18ST_m + 2.98SD + 0.84T_mD \end{cases} \quad (1)$$

The evolution of the exit temperature T_s is plotted as a function of Q_v in Figure 4. The measured value of T_s was lower than the assigned temperature, which is consistent with what has been reported in [17], [18] and [19]. This is due to the fact that the heat transfer between the liquefier walls and the material is insufficient during the residence time for the material to reach its design temperature. At the same time, as Q_v increases, the difference between extrusion temperature T_m and T_s increases. This is because a higher extrusion rate S reduces the residence time of the material in the liquefier, which increases the temperature difference.

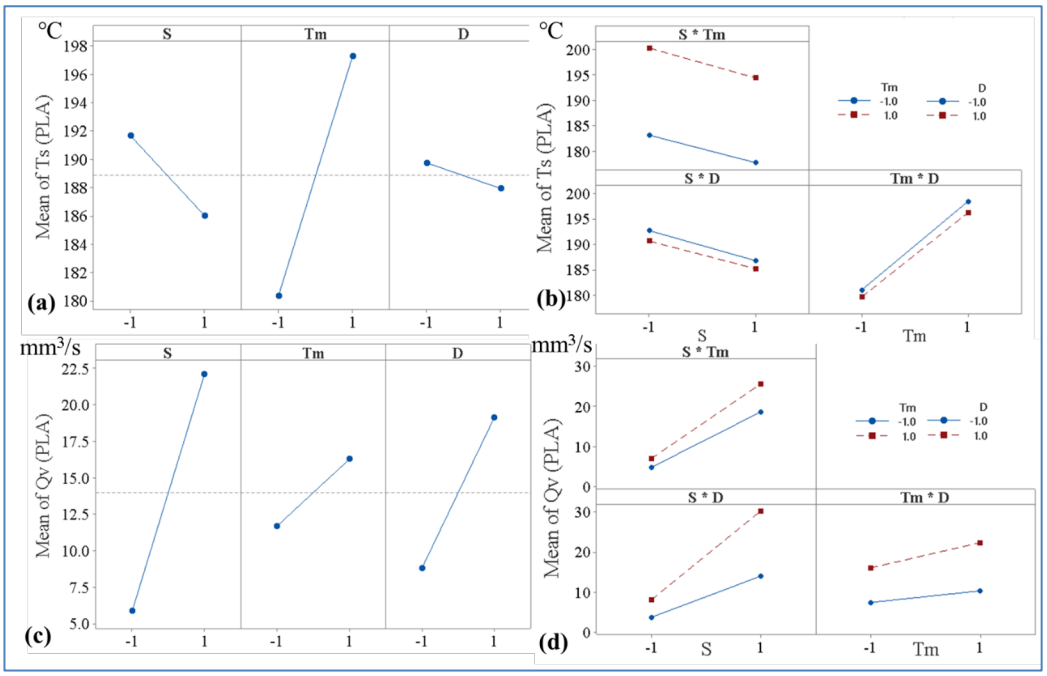

FIGURE 3. (a) Main effects plot for response Ts; (b) Interaction plot for response T_s; (c) Main effects plot for response Q_v; (d) Interaction plot for response Q_v.

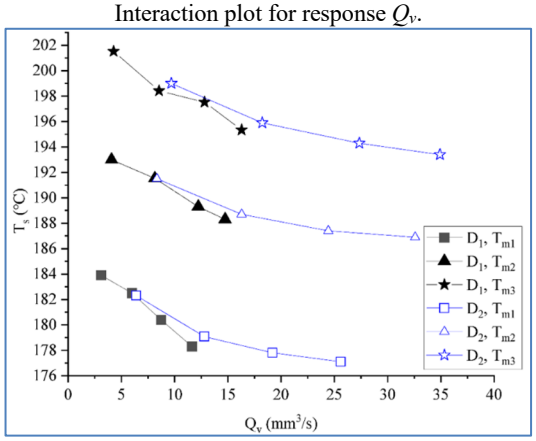

FIGURE 4. The effect of Q_v and T_m on the exit temperature T_s.

SIMULATING POLYMER EXTRUDATE SWELL

Simulating extrudate swell is essential to understand and predict the behavior of PLA during extrusion-based additive manufacturing (MEX). This simulation helps optimize die geometry, processing parameters, and material selection to improve dimensional accuracy. The numerical modeling of PLA extrudate swell is based on continuum mechanics, often involving non-Newtonian fluid flow equations due to the shear-thinning or shear-thickening behavior of polymer melts. Navier-Stokes equations constitutive models are often used to describe the rheological behavior of polymers and simulate the extrusion and swell process. The Level Set (LS) method in COMSOL Multiphysics is a numerical technique used to track interfaces and free surfaces between immiscible fluids [20] and [21]. It is especially useful in simulating die swell during polymer extrusion, where the interface between the polymer and air deforms as the polymer exits the die.

The interface is represented by an iso-contour of a globally defined function, the level set function ϕ. Let be a domain $\Omega(t) \in R^3$ whose boundary Γ is defined by a LS function $\phi(t,x)$. This function is assumed to take the value 1 inside the region bound by the curve Γ and value 0 outside. In order to study the flow in the domain Ω, the LS function divides the domain in two parts $\Omega = \Omega^+ \bigcup \Omega^-$ where:

$$\begin{cases} \phi(t,x)=1 & x\in\Omega^{+} \quad \textit{Inside the polymer} \\ \phi(t,x)=0.5 & x\in\Gamma \quad \textit{Location of the interface}(\textit{polymer / air}) \\ \phi(t,x)=0 & x\in\Omega^{-} \quad \textit{Outside}\ (\textit{air}) \end{cases} \tag{2}$$

If the boundary curve $\Gamma(t,x)$ moves in the normal direction $\vec{n}(t,x)=\dfrac{\vec{\nabla}\phi(t,x)}{\left\|\vec{\nabla}\phi(t,x)\right\|}$ .with velocity $\vec{u}(t,x)$, then the Level

Set function ϕ satisfies the LS equation to solve the advection equation and propagate $\phi=0$ as:

$$\frac{\partial\phi(t,x)}{\partial t}+\vec{u}(t,x).\vec{\nabla}\phi(t,x)=0 \tag{3}$$

Since at time t = 0, $\phi(0,x)=\phi_0$, the initial domain $\Gamma(0)$ is given, as well as its motion in time, it is possible to know the LS function at each time $\phi(t,x)$ using a second-order Runge Kutta scheme in time as follows:

$$\begin{cases} \phi_{t+\Delta t}=\phi_t-\Delta t\left(\vec{u}_t\vec{\nabla}\phi_t\right) \\ \phi_t \quad known \end{cases} \tag{4}$$

The numerical simulations were performed with the Two-Phase Flow solver of LS in COMSOL Multiphysics based on the finite element method. In this study, the compressibility was not considered, therefore, the polymer flow was assumed with assumptions:

1. Incompressible.
2. Laminar flow with negligible inertial forces (stocks flow).
3. Fully developed inside the nozzle.
4. Dissipation effect neglected and isothermal condition inside the nozzle.

The conservation equations can be written as :

$$\begin{aligned} &\vec{\nabla}\cdot\vec{u}=0 \\ &\frac{\partial\vec{u}}{\partial t}=-\frac{1}{\rho}\vec{\nabla}p+\vec{g}+\vec{\nabla}\cdot\left[\eta(\vec{\nabla}\vec{u}+\vec{\nabla}^{T}\vec{u})\right] \\ &\frac{\partial T}{\partial t}+\left(\vec{u}\cdot\vec{\nabla}\right)T=\left(\frac{k}{\rho c_p}\right)\vec{\nabla}^{2}T \end{aligned} \tag{5}$$

where ρ is the fluid density, $\vec{u}$ is the velocity vector, p is the pressure, η is the dynamic viscosity, $\vec{g}$ is the acceleration of gravity, T is the current temperature, k is the thermal conductivity, c_p is the specific heat capacity of the fluid. The term $\alpha=\dfrac{k}{\rho c_p}$ represents the thermal diffusivity within the polymer/air interface defined as:

$$\alpha(\phi)=\phi\alpha_{air}+(1-\phi)\alpha_{polymer} \tag{6}$$

where α_{air} and $\alpha_{polymer}$ represent the diffusivity of the air and the polymer respectively. ϕ is the smooth volume fraction of the fluids varying between 0 and 1 across the free surface and is constant (ϕ = 1 in a PLA domain and ϕ = 0 in an air domain, ϕ = 0.5 is assigned to the polymer air interface).

The LS transport equation 7, which follows the interface between two immiscible fluids are expressed as follows:

$$\frac{\partial\phi}{\partial t}+\vec{\nabla}\cdot(\vec{u}\phi)=\gamma\vec{\nabla}\cdot\left(\varepsilon_{ls}\vec{\nabla}\phi-\phi(1-\phi)\frac{\vec{\nabla}\phi}{\left\|\vec{\nabla}\phi\right\|}\right) \tag{7}$$

where γ is the reset parameter (taken as maximum or close to the maximum fluid velocity to ensure consistency of the simulation results) and ε_{ls} is the parameter controlling the interfacial thickness.

The Simulating Polymer Extrudate Swell is realized by coupling different modules in COMSOL Multiphysics software, as illustrated in Figure 5.

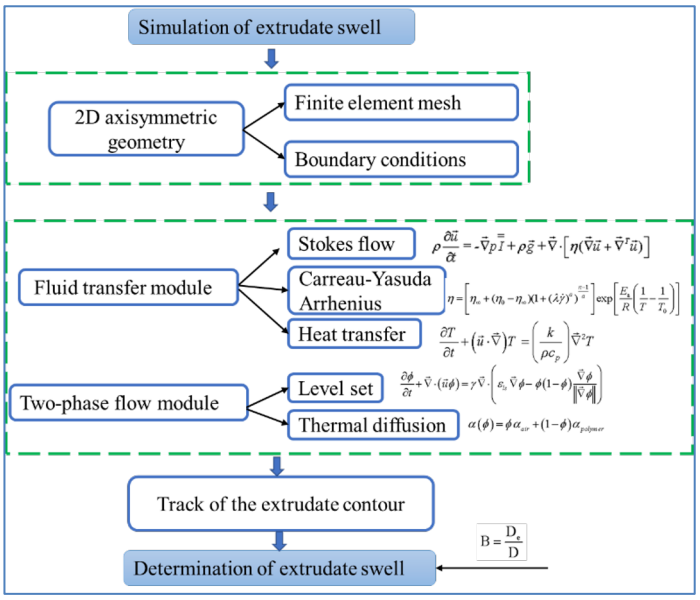

FIGURE 5. Schema of simulation implementation for extrudate swell.

The extrusion simulation of PLA was modeled as 2D axisymmetric, and the geometry is shown in Figure 6. The yellow part is the nozzle channel filled initially by melted polymer and the green part is the air domain where enters then the polymer. The nozzle diameter is $\varnothing D_1 = 0.76$ mm or $\varnothing D_2 = 1.56$ mm. The boundary conditions are shown in Figure 6, including no slip condition and constant extrusion temperature T_m on inner wall of the nozzle, ambient pressure on the outlet and environment temperature $T_{env} = 25°C$) in the air cavity. The mesh size of free triangles is studied and the comparison of element number, calculation time and extrudate swell ratio *B*. The element number and calculation time increase as the mesh size decreases, while the extradate swell ratio *B* decreases to converge to a certain value indicating an increasing accuracy. In order to obtain a relatively high accuracy at a relatively low computational cost, the refined finer mesh configuration is chosen, as shown in Figure 6. The 2D computational grid is physics-controlled meshed (67241 elements) with free triangles and refined in the nozzle contraction region. Finer mesh size is chosen at the polymer-air interface (10138 elements in the Area 1 and 55461 elements in the Area 3) and a very refined mesh (1642 elements) is performed at the exit of the nozzle extruder (Area 2).

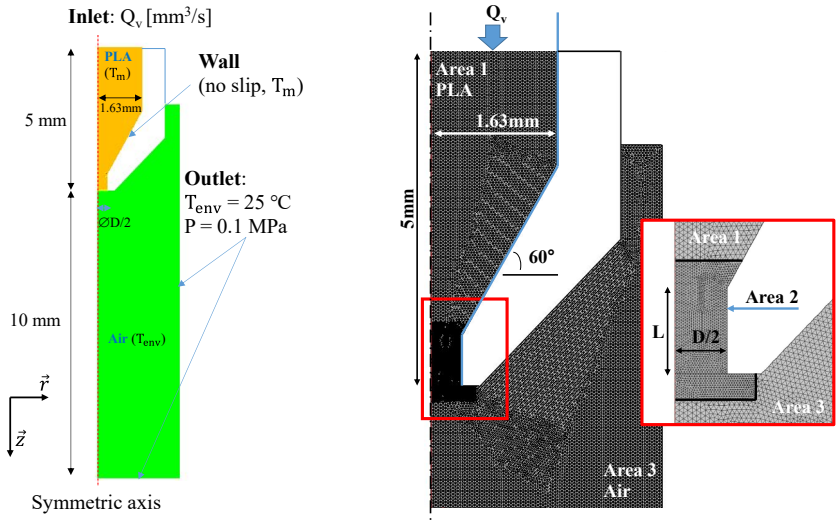

FIGURE 6. Geometry of extrusion simulation model, boundary conditions and 2D mesh.

The simulation for PLA at $T_m = 200°C$, $S_2 = 20$ rpm, and $\varnothing D_1 = 0.76$ mm was conducted with fine mesh size. In our work, the evolution of the volume fraction as a function of time and the comparison of the experimental and numerical profiles are shown in Figure 7. The LS method succeeded in transporting the material to flow as a function of time out of the nozzle. However, the extrudate swell ratio was much higher (> 60%) than experimental result,

which is due to the inappropriate mesh size and dependent interface thickness of LS method shows the evolution of swell ratio characterized at 2 mm below the nozzle exit as a function of time. The swell ratio tends to a constant value after t = 0.9 s, indicating that the gravity effect has insignificant effect on the die swell in this regime. The swell ratio in simulation is measured at t = 1 s.

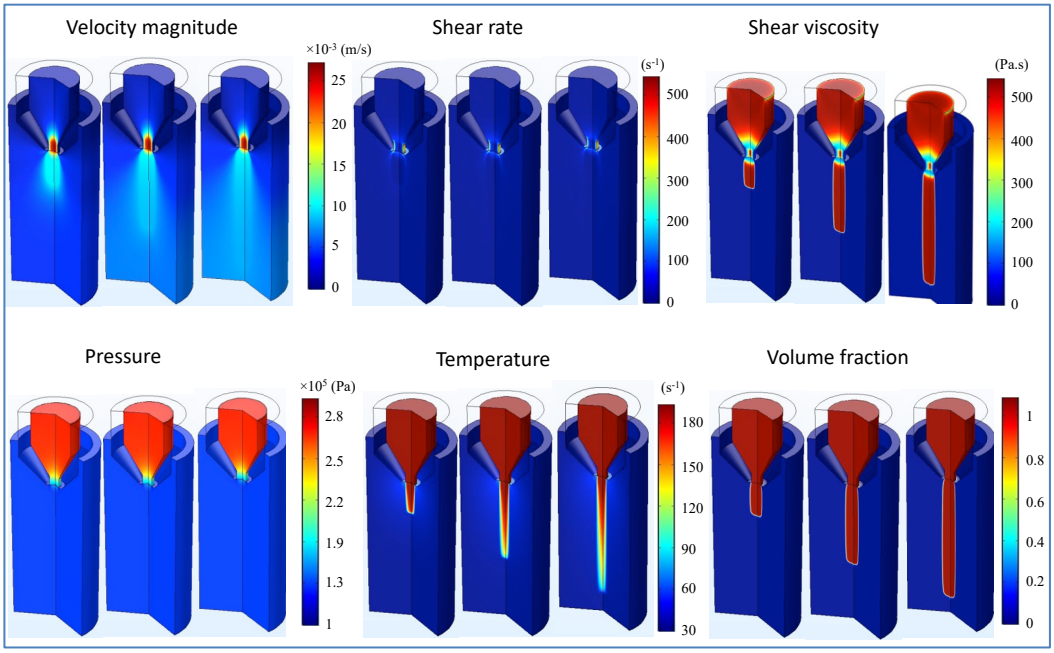

Figure **8.** Physical fields of PLA extrusion ($Tm2$ = 200 °C, $\varnothing D1$ = 0.76 mm and S2 = 20 rpm at t = 0.2 s, 0.6 s and 1 s).

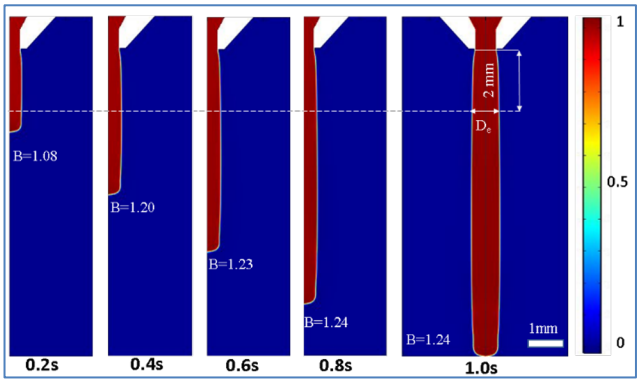

FIGURE 7. Transient behavior of the extrudate at T_{m2}, $\varnothing D_1$ and S_2.

The evolution of physical fields as a function of time for PLA is given in Figure 8. These physical parameters change dramatically at the nozzle contraction region. For instance, in the vertical flow direction, the velocity magnitude of the material increases and then decreases when it pass through the contraction region and the nozzle head. From the nozzle center to the wall, i.e., perpendicular to the flow direction, the velocity magnitude decreases from maximum to zero (no slip boundary condition).

Figure 9 compares the swell ratio between experimental and numerical results as a function of the Q_v at T_{m2}, which shows that the swell ratio increases with increasing Q_v for both nozzles. The nozzle of larger diameter has lower swell ratio, which is in accordance with literature [12]. The experimental and numerical results at T_{m2} are summarized in Tables 3 and 4. The numerical error is within 4%.vThe obtained results show that the swell ratio decreases with increasing T_m, which can be explained by the effect of temperature on the polymer chain mobility that a higher temperature promotes the movement of polymer chains and contributes to their reorientation and release of deformation resulted from the shear and compression forces in extrusion. The deviation between the simulation results and experimental results is within 3%. According to the above results, it can be concluded that reducing the

extrusion swell can be achieved by decreasing S, increasing T_m and $\varnothing D$, but the printing speed and dimensional resolution should be considered. The numerical model can be used to predict the extrudate swelling whereas an overestimation for powder filled polymers occurs, which requires further modeling on the constitutive behavior of two phases system.

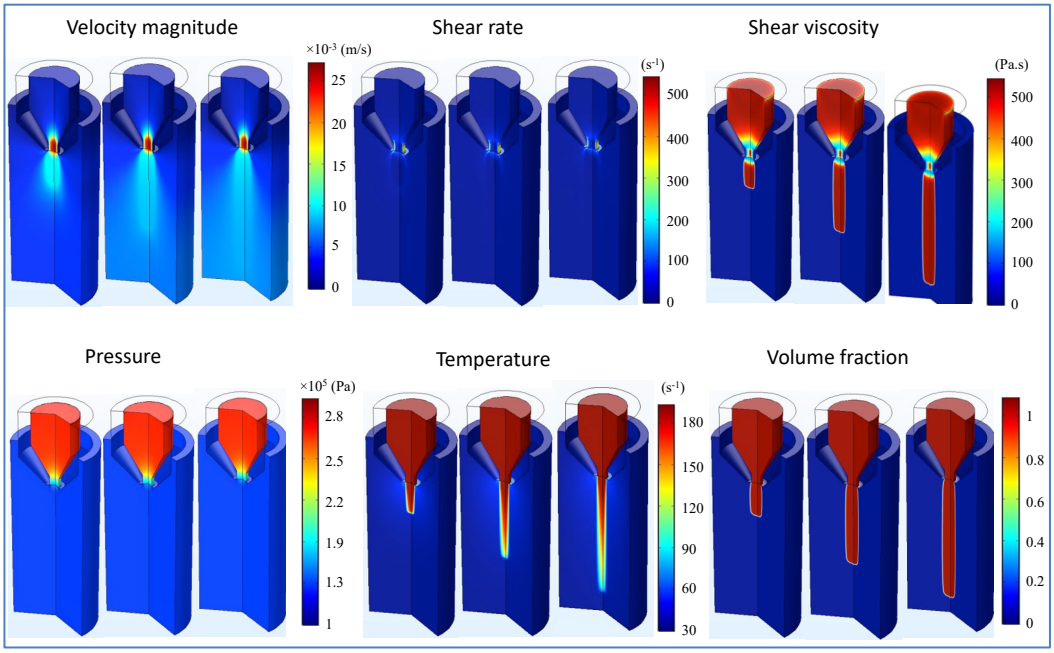

FIGURE 8. Physical fields of PLA extrusion (T_{m2} = 200 °C, $\varnothing D_1$ = 0.76 mm and S_2 = 20 rpm at t = 0.2 s, 0.6 s and 1 s).

TABLE 3. Comparison of extrudate swell ratio for PLA at temperature T_{m2} for PLA with nozzle diameter $\varnothing D_1$.

Volume flow rate Q_v (mm³/s)	Experiment swell ratio	Simulation swell ratio	Error (%)
4.07	1.18	1.19	0.85
8.15	1.22	1.24	1.64
12.22	1.23	1.27	3.25
14.74	1.24	1.27	2.42

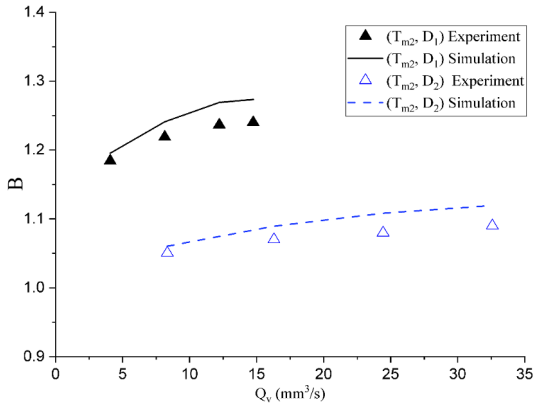

FIGURE 9. Experimental and simulation comparison of die swell at different Q_v and at T_{m2}.

TABLE 4. Comparison of extrudate swell ratio for PLA at temperature T_{m2} for PLA with nozzle diameter $\varnothing D_2$.

Volume flow rate Q_v (mm^3/s)	Experiment swell ratio	Simulation swell ratio	Error (%)
8.34	1.05	1.06	0.95
16.29	1.07	1.09	1.81
24.44	1.08	1.11	2.64
32.58	1.09	1.12	2.68

TABLE 5. Comparison of extrudate swell ratio between experimental and numerical results at extrusion temperature T_{m1} and T_{m3} with fixed nozzle diameter $\varnothing D_1$ = 0.76mm and S_3 = 30 rpm.

	T_{m1} = 190°C	T_{m3} = 210°C
Experiment swell ratio	1.24	1.18
Simulation swell ratio	1.27	1.20
Error (%)	2.66	1.80

CONCLUSION

In this study, a comprehensive investigation was conducted to explore the extrusion process of polylactic acid (PLA). The primary objective of the research was to investigate the impact of nozzle geometry, processing parameters, and material properties on the extrudate swell. The experimental characterization of extrudate swell was conducted using a dynamic camera to capture the evolution of the extrudate profile in real-time. The impact of extrusion temperature, nozzle diameter, and extrusion rate on the volume flow rate were analyzed. The numerical simulation was performed in COMSOL Multiphysics software using the Level Set Two-Phase flow module with thermal coupling. Following the optimization of mesh size, the simulations revealed the distribution of velocity, pressure, and shear rate, viscosity, and temperature within and outside the nozzle. It was observed that the extrudate undergoes a rapid and significant swelling right out of the nozzle exit and tends to equilibrate between the swelling behavior and the tension forces from the hanging mass.

REFERENCES

1. Ramazani H, Kami A (2022) Metal FDM, a new extrusion-based additive manufacturing technology for manufacturing of metallic parts: a review. Prog Addit Manuf 7:609–626. https://doi.org/10.1007/s40964-021-00250-x
2. W. Sinthavathavorn, M. Nithitanakul, B. P. Grady, and R. Magaraphan, “Melt rheology and die swell of PA6/LDPE blends by using lithium ionomer as a compatibilizer,” Polym. Bull., vol. 63, no. 1, pp. 23–35, Jul. 2009, doi: 10.1007/s00289-009-0063-x.
3. J. Z. Liang, J. Yang, and C. Y. Tang, “Die-swell behavior of PP/$Al(OH)_3$/$Mg(OH)_2$ flame retardant composite melts,” Polym. Test., vol. 29, no. 5, pp. 624–628, 2010, doi: 10.1016/j.polymertesting.2010.03.014.
4. J. S. Anand and I. S. Bhardwaj, “Die swell behaviour of polypropylene - An experimental investigation,” Rheol. Acta, vol. 19, no. 5, pp. 614–622, Sep. 1980, doi: 10.1007/BF01517515.
5. E. Behzadfar, M. Ansari, V. K. Konaganti, and S. G. Hatzikiriakos, “Extrudate swell of HDPE melts: I. Experimental,” J. Nonnewton. Fluid Mech., vol. 225, pp. 86–93, Nov. 2015, doi: 10.1016/j.jnnfm.2015.07.008.
6. L. A. Utracki, Z. Bakerdjian, and M. R. Kamal, “A method for the measurement of the true die swell of polymer melts,” J. Appl. Polym. Sci., vol. 19, no. 2, pp. 481–501, Feb. 1975, doi: 10.1002/app.1975.070190213.
7. A. Dutta and M. E. Ryan, “A study of parison development in extrusion blow molding,” J. Nonnewton. Fluid Mech., vol. 10, no. 3–4, pp. 235–256, Jan. 1982, doi: 10.1016/0377-0257(82)80003-7.
8. D. Kalyon, V. Tan, and M. R. Kamal, “The dynamics of parison development in blow molding,” Polym. Eng. Sci., vol. 20, no. 12, pp. 773–777, Aug. 1980, doi: 10.1002/pen.760201202.
9. Y. Béreaux, J.-Y. Charmeau, and J. Balcaen, “Optical measurement and modelling of parison sag and swell in blow moulding,” Int. J. Mater. Form., vol. 5, no. 3, pp. 199–211, Sep. 2012, doi: 10.1007/s12289-011-1040-0.
10. D. Tang, F. H. Marchesini, D. R. D’hooge, and L. Cardon, “Isothermal flow of neat polypropylene through a slit die and its die swell: Bridging experiments and 3D numerical simulations,” J. Nonnewton. Fluid Mech., vol. 266, no. December 2018, pp. 33–45, 2019, doi: 10.1016/j.jnnfm.2019.02.004.
11. R. I. Tanner, “A theory of die-swell,” J. Polym. Sci. Part A-2 Polym. Phys., vol. 8, no. 12, pp. 2067–2078, Dec. 1970, doi: 10.1002/pol.1970.160081203.
12. D. Tang, F. H. Marchesini, L. Cardon, and D. R. D’hooge, “Three-dimensional flow simulations for polymer extrudate swell out of slit dies from low to high aspect ratios,” Phys. Fluids, vol. 31, no. 9, p. 093103, Sep. 2019, doi: 10.1063/1.5116850.

13. V. K. Konaganti, M. Ansari, E. Mitsoulis, and S. G. Hatzikiriakos, “Extrudate swell of a high-density polyethylene melt: II. Modeling using integral and differential constitutive equations,” J. Nonnewton. Fluid Mech., vol. 225, pp. 94–105, Nov. 2015, doi: 10.1016/j.jnnfm.2015.07.005.
14. R. V. Morgan, R. S. Reid, A. M. Baker, and D. Bernardin, John, “Emissivity Measurements of Additively Manufactured Materials,” Los Alamos Natl. Lab. (LANL), Los Alamos, NM (United States), no. LA-UR-17-20513, 2017.
15. B. Wijnen, P. Sanders, and J. M. Pearce, “Improved model and experimental validation of deformation in fused filament fabrication of polylactic acid,” Prog. Addit. Manuf., vol. 3, no. 4, pp. 193–203, Dec. 2018, doi: 10.1007/s40964-018-0052-4.
16. M. Hyvärinen, R. Jabeen, and T. Kärki, “The Modelling of Extrusion Processes for Polymers—A Review,” Polymers, vol. 12, no. 6, p. 1306, Jun. 2020, doi: 10.3390/polym12061306.
17. D. A. Anderegg et al., “In-situ monitoring of polymer flow temperature and pressure in extrusion based additive manufacturing,” Addit. Manuf., vol. 26, no. January, pp. 76–83, 2019, doi: 10.1016/j.addma.2019.01.002.
18. M. P. Serdeczny, R. Comminal, D. B. Pedersen, and J. Spangenberg, “Experimental and analytical study of the polymer melt flow through the hot-end in material extrusion additive manufacturing,” Addit. Manuf., vol. 32, no. October 2019, p. 100997, Mar. 2020, doi: 10.1016/j.addma.2019.100997.
19. A. Dervieux and F. Thomasset, “A finite element method for the simulation of a Rayleigh-Taylor instability,” in Approximation Methods for Navier-Stokes Problems, Berlin, Heidelberg: Springer, 1980, pp. 145–158.
20. S. Osher, R. Fedkiw, and K. Piechor, “Level Set Methods and Dynamic Implicit Surfaces,” Appl. Mech. Rev., vol. 57, no. 3, pp. B15–B15, May 2004, doi: 10.1115/1.1760520.
21. J. A. Sethian, Level Set Methods and Fast Marching Methods: Evolving Interfaces in Computational Geometry, Fluid Mechanics, Computer Vision, and Materials Science. Cambridge University Press, 1999.